Study of the Mechanism of Carbonization of Template in Silicon-Substituted Aluminophosphate Zeolite Crystals

Jian Pang Zhai,[†] Wei Wei Peng,[‡] Irene Ling Li,[†] Shuang Chen Ruan,[†] and Zi Kang Tang*[,‡]

College of Electronic Science and Technology, Shenzhen University, Shenzhen, 518060, People's Republic of China, and Department of Physics, Hong Kong University of Science and Technology, Clear Water Bay, Kowloon, Hong Kong, People's Republic of China

Received: March 12, 2008; Revised Manuscript Received: June 1, 2008

Silicon-substituted microporous aluminophosphate $AlPO_4$-11 zeolite crystals (SAPO-11) were synthesized by a hydrothermal method. The dipropylamine (DPA) molecules were incorporated in the one-dimensional channels of SAPO-11 as organic templates. The DPA molecules can be pyrolyzed at high temperature, and form 0.3 nm single-walled carbon nanotubes (SWNTs). The detailed carbonization process of DPA molecules has been investigated by using Fourier transform infrared measurements (FTIR), mass spectrometry, thermogravimeter (TG), and micro-Raman spectroscopy. During the pyrolysis process, the DPA molecules decompose into propylene and ammonia at 673 K, and then the C−H bonds of C_3H_6 start to break when temperature is above 698 K. The 0.3 nm SWNTs are formed sequentially in the channels of SAPO-11 crystals at about 723 K.

1. Introduction

Since the first report of carbon nanotubes,[1] many research works have been carried out in the past decade due to their novel properties and many potential applications. The control of chirality, diameter, and alignment of nanotubes has been crucial for both applications and experiments aimed at clarifying their physical characteristics. In 1998, Tang et al. reported a new technique to fabricate monosized ultrathin, single-walled carbon nanotubes (SWNTs) with a diameter as small as 0.4 nm, using $AlPO_4$-5 zeolite (structure code AFI) crystals as the template.[2–4] Those ultrathin SWNTs constitute the best example of quasi-one-dimensional (1D) quantum wires, and show peculiar physical properties, which are not predicted in SWNTs with large diameter.[5–8] Calculations based on energetic considerations have shown that free-standing SWNT with a diameter of 0.4 nm is only marginally stable thermodynamically.[9] Because the cohesive energy of 0.3 nm SWNTs is positive, they cannot exist in the free-standing state. The unstable carbon nanotubes can, however, be stabilized in a geometrically constrained environment. For example, 0.3 nm carbon nanotubes have been found stable as the central shell of a multiwalled carbon nanotube.[10] Thus template method with use of zeolite is a powerful technique to synthesize 0.3 nm SWNTs.

We have tried several possible zeolite structures and found a new type of zeolite Si-substituted $AlPO_4$-11 (SAPO-11) crystals that is a good template for synthesizing 0.3 nm SWNTs.[11] Figure 1 shows the model of a SAPO-11 crystal viewed along the (001) direction. The framework of the SAPO-11 crystal consists of alternating tetrahedral $(AlO_4)^-$ and $(PO_4)^+$, which form a 1-D elliptical channel system. The diameters of the major and minor axes are 4.3 and 6.5 Å.[12] The ultrathin SWNTs are synthesized by pyrolyzing organic template molecules of dipropylamine (DPA) that are incorporated into the channels in a vacuum of 10^{-3} mbar. The periodic structures of zeolite crystals make it possible to build a quasi-3D structure for carbon nanotubes that is of importance for making optical and transport devices as it is. Both for fundamental research and practical applications, synthesis of high-quality 0.3 nm SWNTs in SAPO-11 crystal channels is essential. However, a significant number of organic template molecules can escape from the channels during the pyrolysis process, leading to increased structural defects. As the structural quality of the SWNTs would greatly affect the physical properties of the nanotube-zeolite composite, the understanding of the pyrolyzing process of DPA molecules is important for us to optimize synthesis conditions and improve the quality of 0.3 nm nanotubes.

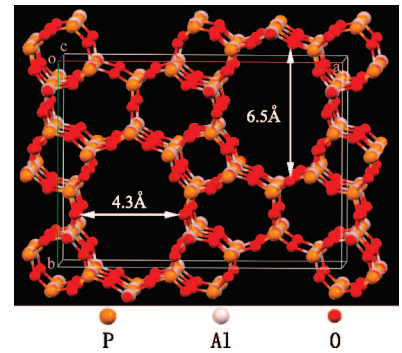

Figure 1. Model of the SAPO-11 crystal viewed along the (001) direction.

In this paper, we in situ monitor the carbonization process of DPA in SAPO-11 crystals by a combined technique of Fourier transform infrared measurements (FTIR), mass spectrometry, thermogravimeter (TG), and micro-Raman spectroscopy. The monitored temperature range is from 300 to 873 K. The carbonization process of the DPA molecules (in the channels of SAPO-11 crystals) has been observed to consist of stepped decomposition into lighter amines through the sequential abstraction of propylene, in the temperature range of 648−698 K. Micro-Raman measurements show the 0.3 nm nanotubes to be formed at about 723 K.

* Corresponding author. E-mail: phzktang@ust.hk.
[†] Shenzhen University.
[‡] Hong Kong University of Science and Technology.

10.1021/jp802218x CCC: $40.75
Published on Web 07/16/2008

2. Experimental Section

2.1. Synthesis of SAPO-11 Crystals. SAPO-11 crystals were synthesized by using a hydrothermal method. Detailed synthesis procedures have been reported elsewhere.[13] Briefly, Aluminum triisopropoxide [(iPrO)$_3$Al] and phosphoric acid (H_3PO_4 85 wt %) were used as aluminum and phosphorus sources, respectively. Carbon precursor of DPA was employed as the organic template for SAPO-11 hydrothermal growth. The starting gel consisted of the composition 0.05Si:1.0Al_2O_3:1.0P_2O_5:1.2 DPA:400H_2O. The aluminum triisopropoxide and fumed silica were hydrolyzed in water, followed by the dropwise addition of H_3PO_4 with vigorous stirring. The organic template was slowly added to the viscous aluminophosphate gel. The gel formed from the reaction mixture was sealed in a Teflon-lined stainless autoclave and heated to 458 K under autogenous pressure for 30 h. Finally, the solid products were filtered and washed with distilled water. SAPO-11 crystals were then obtained.

2.2. Characterization. Fourier transform infrared (FTIR) spectra were recorded with a FTIR spectrometer (Bio-Rad FTS 6000) for in situ monitoring the pyrolysis process of carbon precursor DPA (in the channels) at various temperatures. The decomposition products escaping from the SAPO-11channels were identified by interfacing a temperature programmable furnace to a mass spectrometer (ABB MS250, Extrel Corporation, USA). To avoid the influence of the physisorbed water inside the channels of crystals, the as-synthesized sample was first treated under the vacuum of 10^{-3} mbar at 373 K for 3 h. After the water was desorbed, these crystals were heated at 3 deg/min from 373 to 873 K. Adequate sensitivity was obtained with 5 g of sample. The weight loss process of the organic template in the channels was recorded with a thermal analysis apparatus (STA 449C Jupiter). The mass resolution of the equipment was 0.1 μg. Sample was heated at 3 deg/min from room temperature to 873 K. Raman spectra of the DPA@SAPO-11 crystals were measured by using a Jobin Yvon-T64000 micro-Raman spectrometer, with the 514.5 nm line of an Ar−Kr ion laser as the excitation. The equipped CCD detector was cooled by liquid nitrogen.

3. Results and Discussion

Organic template molecules DPA are oriented in a head-tail manner in the 10-ring channels of SAPO-11 crystals. Mali and Han et al. have reported that the organic template DPA is protonated in the channels of $AlPO_4$-11 crystals.[14,15] Thus, it can be expected that the organic DPA is also protonated inside the channels of SAPO-11 crystals. The DPA molecules exist in the channels of SAPO-11 crystals in the form of dipropylammonium hydroxide ($(CH_3CH_2CH_2)_2NH_2^+OH^-$) if the crystals are synthesized from a gel without F^-, or in the form of dipropylammonium fluoride ($(CH_3CH_2CH_2)_2NH_2^+F^-$) from a starting gel with F^- ions, and the form of $(CH_3CH_2CH_2)_2NH_2^+Z^-$, where Z^- is the negatively charged framework, which is induced by replacement of partial P^{5+} irons with Si^{4+} irons in the SAPO-11 crystal.[16,17] These predominating forms are similar to that of TPA in AFI crystals.[18] We study the carbonization process of DPA occluded within SAPO-11 crystals prepared without F^-. Thus, there are two predominating forms in the crystal channels: $(CH_3CH_2CH_2)_2NH_2^+OH^-$ and $(CH_3CH_2CH_2)_2NH_2^+Z^-$.

To study the decomposition process of dipropylammonium ions in the channels of SAPO-11 crystals, 0.5 mg of crystal powder was pressed into a tablet and put on a temperature-controlled holder for in situ FTIR spectral measurement with continuously flowing nitrogen stream. The temperature was varied from 300 to 823 K. Figure 2 shows the FTIR spectra in the frequency region 2000−4000 cm^{-1}. At room temperature, the spectrum exhibits three main features: (1) The peaks in the region 2000−2600 cm^{-1} are due to the overtones plus their combinations of the Al−O−P vibrations (from crystal framework). (2) The peaks in the region 2600−3400 cm^{-1} are due to the DPA molecules. (3) The peaks in the region 3400−3700 cm^{-1} are due to the O−H vibration.[19] With increasing temperature, the relative intensity of the O−H band weakens, becoming undetectable above 573 K, implying desorption of water. We can thus assume that dipropylammonium hydroxide ($(CH_3CH_2CH_2)_2NH_2^+OH$ has been partially converted to $(CH_3CH_2CH_2)_2NH$ at this temperature. With further increasing the temperature to 723 K, the relative intensity of the N−H peaks (3053−3307 cm^{-1}) and the C−H peak at 2885 cm^{-1} decrease and vanish. This implies that the thermal treatment leads to the decomposition of the $(CH_3CH_2CH_2)_2NH_2^+$ ion by sequential abstraction of propylene (C_3H_6), with stepwise formation of n-propylammonium ion $(CH_3CH_2CH_2)NH_3^+$ and ammonia molecules (NH_3). At even higher temperature, the C−H vibration signals at 2941 and 2978 cm^{-1} become weaker and finally undetectable when the sample is heated to 823 K. This indicates that at this temperature, the C−H bonds of C_3H_6, or its smaller oligomers, start to break. Noteworthy is that two new bands at wavenumbers higher than 3500 cm^{-1} are observed at a temperature of 723 K. The vibration band at 3576 cm^{-1} is probably characteristic of the OH group interacting additionally with the framework oxygen atoms. The band at 3745 cm^{-1} is assigned to isolated Si−OH−Al groups. This is because the substitutions of Si for P in the framework result in the formation of two new O−H stretching vibrations.[19]

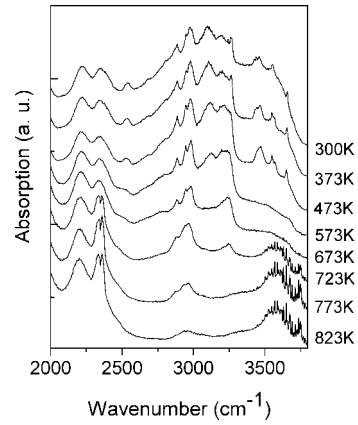

Figure 2. FTIR spectra of SAPO-11 crystals containing DPA, recorded at various temperature under a nitrogen atmosphere.

FTIR spectra can only monitor the decomposition process that occurs inside the crystal channels, but cannot identify the gas species that escape from the channels. The use of a mass spectrometer remedies this situation. The mass spectra recorded at different temperatures are shown in Figure 3. By elevating the temperature to 473 K, an increasing intensity of water signals (m/z 18 and 17) is observed without other gas signals indicating the H_2O moisture is released. The presence of new m/z signals at 101, 72, and 30 is attributable to the formation of neutral DPA, and these signals increases gradually with an increase in the temperature from 498 to 623 K. H_2O is the first species observed, presumably because it diffuses more rapidly through the zeolite channels than that of the neutral DPA molecules.

$$(CH_3CH_2CH_2)_2NH_2^+OH^- \rightarrow (CH_3CH_2CH_2)_2NH + H_2O$$

(473 K)

On heating to 673 K, the signals at *m*/*z* 42, 41, 39, and 27 are observed, which are characteristic of propylene (C_3H_6), indicating that the $(CH_3CH_2CH_2)_2NH_2^+$ ion decomposes to the lower ammonium ion $(CH_3CH_2CH_2)NH_3^+$ and propylene. The spectra recorded between 673 and 698 K indicate the decomposition of the lower ammonium ion $(CH_3CH_2CH_2)NH_3^+$ to propylene and ammonia (NH_3). This is evidenced by the signals at 42, 41, 39, and 27 due to propylene and the signals at 17 and 16 due to ammonia. A similar mechanism has been reported by Soulard, Nowotny and Park et al.,[20–22] who investigated decomposition of tetrapropylammonium cations inside the channels of ZSM-5 crystals.

$$(CH_3CH_2CH_2)_2NH_2^+Z^- \rightarrow (CH_3CH_2CH_2)NH_3^+Z^- + C_3H_6$$

(648 − 698 K)

$$(CH_3CH_2CH_2)NH_3^+Z^- \rightarrow NH_3 + C_3H_6 + H^+Z^-$$

The signals at *m*/*z* 91, 92, 105, and 106 are observed when the sample is heated to 723 K. These are characteristics of xylene species. The mass spectral data (*m*/*z* 72, 57, 56, 55, 43, 42, 41, 39, 29, and 27) confirm that 2-methylbutane (C_5H_{12}) is also produced, and suggest that propane and butane may also have been produced. It is possible that part of the catalytic activity is responsible for this.[23] The signals of 2-methylbutane become weaker and finally undetectable when the sample is heated to 773 K, while the intensities of H_2 (*m*/*z* 2) and C_2H_4 (*m*/*z* 28, 27, and 26) are still observed. With further increase of temperature, the intensities of all the above-mentioned signals decease, and finally become negligible when the heating temperature reaches 873 K or above.

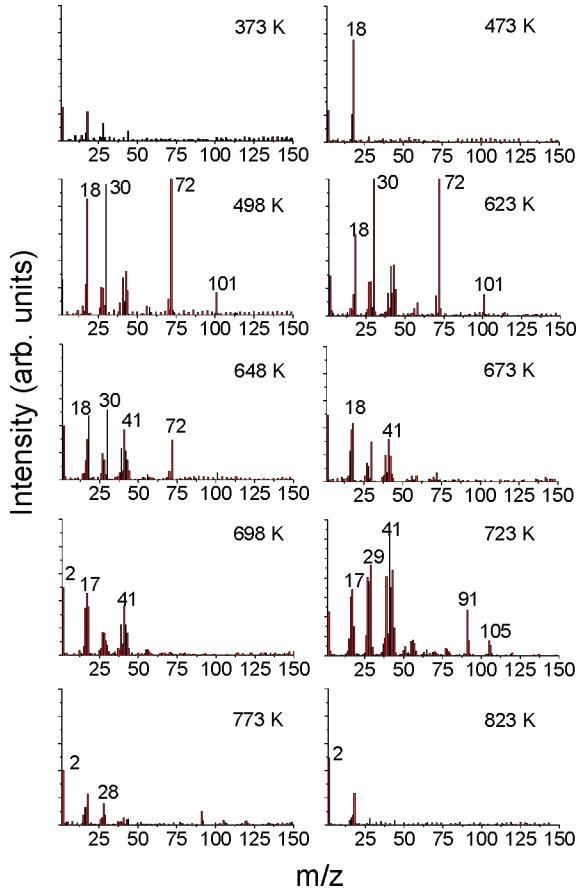

Figure 3. Mass spectra obtained at various points during the thermal pyrolysis of organic template occluded within SAPO-11 crystals in the temperature range 373−823 K.

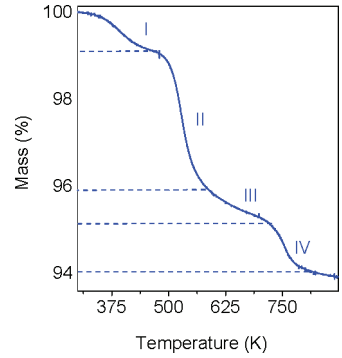

Figure 4. TG curves measured at temperatures ranging from 390 to 873 K.

$$C_3H_6 \rightarrow 3C + 3H_2\uparrow \quad (above\ 698\ K)$$

The pyrolysis process of DPA inside the channels of SAPO-11 crystals was further monitored by a TG analyzer. In the experiment, we kept the sample in the environment under continuous helium stream, and carefully dehydrated the samples at 383 K to eliminate the influence of physisorbed water in the crystals. Figure 4 shows the measured TG curve, which can be cataloged into four distinct temperature regions denoted by I to IV. In region I (390−490 K), the weight loss is due to the evaporation of the water resulting from the conversion of $(CH_3CH_2CH_2)_2NH_2^+OH^-$ to $(CH_3CH_2CH_2)_2NH$ and H_2O. In region II (490−590 K), the weight loss can be attributed to the volatile vaporization of $(CH_3CH_2CH_2)_2NH$ molecules, which is in agreement with the mass spectra measured in the same temperature region (see Figure 3). The weight loss in region III (590−730 K) is due to the small molecules from the $(CH_3CH_2CH_2)_2NH_2^+Z^-$ by breaking the C−N band. In this region, the pyrolysis temperature is high enough to break C−N bands, but not C−H bands. Decomposition of $(CH_3CH_2CH_2)_2NH_2^+Z^-$ leads to the successive release of propylene and ammonia molecules. The weight loss in the final region IV (730−873 K) can be attributed to the degradation of the propylene molecules, where the C−C and C−H bonds of C_3H_6 start to break and small molecules such as H_2, CH_4, and C_2H_2 are generated.

To study the carbonization process of the DPA molecules in the SAPO-11 crystal channels, we measured the Raman spectra of DPA@SAPO-11 crystals during the pyrolysis process (in the temperature range 300−773 K). The result is shown in Figure 5. At room temperature, the curve shows typical characteristic Raman-active modes for DPA molecules. The peak at about 1462 cm^{-1} is assigned to the CH_3 antisymmetrical deformation mode. The peak near 967−1150 cm^{-1} is attributed to the C−N stretching mode.[24] The Raman signals at frequencies of 449 and 494 cm^{-1} can originate from deformations of four T-atom-membered rings of the SAPO-11 framework.[25] All signals related to DPA molecules disappear from the spectrum when the sample is heated above 673 K. This implies that the carbon precursor DPA molecules start to decompose at this temperature. By elevating temperature up to 723 K, the *G*-band at 1600 cm^{-1} and RBM at 760 cm^{-1} are observed, implying that carbon atoms are graphitized in the channels. As a result, the color of crystal changes from transparent to black with a significant amount of optical anisotropy, indicating transformation of nanostructures

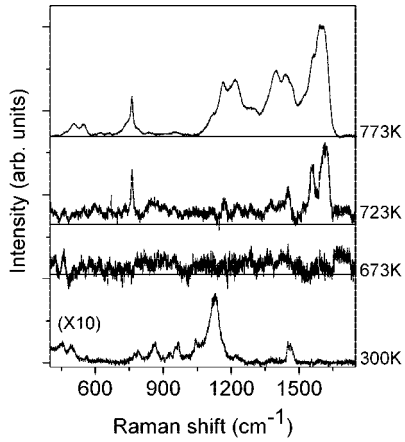

Figure 5. Raman spectra of the DPA contained inside the channels of SAPO-11 crystal were measured at various temperatures in a vacuum of 10^{-3} mbar.

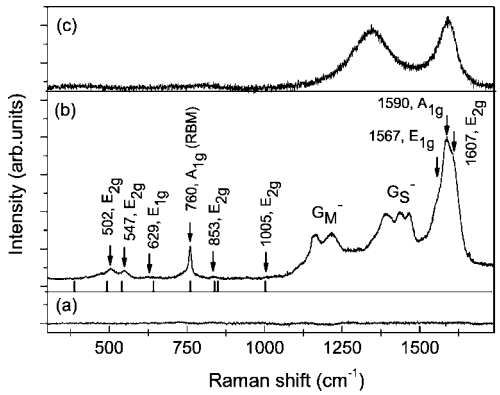

Figure 6. (a) Raman spectrum of a calcined SAPO-11 crystal. (b) Raman spectrum of a SWNT@SAPO-11 crystal. (c) Raman spectrum of the carbon specimen after removing the zeolite framework.

inside the channels from disordered to ordered carbon structures. The 0.3 nm carbon nanotubes appear at this temperature. At even higher temperatures, the relative intensity of the *G*-band gradually increases.

Figure 6b shows the Raman spectrum of SWNTs @SAPO-11. In general, the Raman spectrum exhibits two main features: (1) In the low-frequency region (300−1100 cm^{-1}), there exists a strong characteristic radial-breathing-mode (RBM) at 760 cm^{-1} together with some weak features of vibration modes. (2) The tangential graphite-like G-band that is splitted into G^+ modes in the high-frequency region (1550−1620 cm^{-1}) and G^- modes in the intermediate frequency region (1110−1500 cm^{-1}). Considering the van der Waals radius of the carbon atom and the dimension of the elliptical channel, the diameter of the nanotube in the channel of the SAPO-11 crystal would not be larger than 0.3 nm. There are three possible structures for SWNTs with a diameter of about 0.3 nm: the armchair (2,2), the chiral (3,1), and the zigzag (4,0) nanotubes. To understand the structure of 0.3 nm SWNTs, we calculated vibration modes for (4,0), (3,1) and (2,2) nanotube structures based on a density function approximation.[26,27] The Raman-active modes in the low-frequency region calculated for the (2,2) tube are shown by the vertical bars. The calculated Raman-active modes of the (2,2) tube are in good agreement with the frequencies observed in the Raman spectrum. In particular, the calculated vibration frequency of the RBM of the (2,2) is 760 cm^{-1}. The RBM frequency observed in the Raman spectrum agrees exactly with that calculated for the (2,2) nanotubes. The vibration frequency of the characteristic RBM of the (4,0) and the (3,1) are 620 and 663 cm^{-1}, respectively. Our calculation result is consistent with those reported in the literatures.[28,29] Polarized and resonant characteristics of the Raman scattering combined with a first-principle calculation also revealed that 0.3 nm SWNTs formed inside the elliptical channels of the SAPO-11 crystals have (2,2) armchair symmetry. Detailed investigation of Raman scattering and the first-principle simulation will be published elsewhere.

As a reference, the Raman spectrum of a calcined SAPO-11 crystal is shown as well. As shown in Figure 6a, all the signals of SWNTs disappeared after the sample was burned in air. We also measured the Raman spectrum of the carbon specimen after removing the zeolite framework using HCl acid. As shown in Figure 6c, only the signals of amorphous carbon are detected when nanotubes are exposed in free space, indicating that the freestanding 0.3 nm SWNTs are below the stability limit due to the strong curvature effect induced by their ultrasmall diameter. All these results further confirm that the 0.3 nm nanotubes are formed inside the channels of zeolite crystals.

4. Conclusions

We presented a detailed study of the carbonization process of DPA occluded within SAPO-11 crystals. The dipropylammonium ion is bonded to the framework and its decomposition undergoes a series of reactions to give propylene and ammonia, with the stepwise formation of *n*-propylammonium cations. The 0.3 nm nanotubes are formed at about 723 K.

Acknowledgment. The authors are grateful to Professor P. Sheng for many useful discussions. This research was supported by Hong Kong CERGC Grants of 602807, HKUST President Direct Allocation F0204-A, and the SZU R/D Fund (200849). Dr I. L. Li is thankful for the financial support from NSFC (10704050) and the Huo Ying Dong Educational Foundation (114009).

References and Notes

(1) Iijima, S. *Nature.* **1991**, *354*, 56.
(2) Tang, Z. K.; Sun, H. D.; Wang, J.; Chen, J.; Li, G. *Appl. Phys. Lett.* **1998**, *73*, 2287.
(3) Sun, H. D.; Tang, Z. K.; Chen, J.; Li, G. *Appl. Phys. A* **1999**, *69*, 381.
(4) Wang, N.; Tang, Z. K.; Li, G. D.; Chen, J. S. *Nature* **2000**, *408*, 50.
(5) Tang, Z. K.; Zhang, L.; Wang, N.; Zhang, X. X.; Wen, G. H.; Li, G. D.; Wang, J. N.; Chan, C. T.; Sheng, P. *Science* **2001**, *292*, 2462.
(6) Guo, J. D.; Yang, C. L.; Li, Z. M.; Bai, M.; Liu, H. J.; Li, G. D.; Wang, E. G.; Chan, C. T.; Tang, Z. K.; Ge, W. K.; Xiao, X. D. *Phys. Rev. Lett.* **2004**, *93*, 017402.
(7) Mei, Y. F.; Siu, G. G.; Fu, R. K. Y.; Chu, P. K.; Li, Z. M.; Zhai, J. P.; Liu, H. J.; Tang, Z. K.; Tang, L. C. W.; Ong, H. C. *Appl. Phys. Lett.* **2005**, *87*, 213114.
(8) Liu, H. J.; Li, Z. M.; Liang, Q.; Tang, Z. K.; Chan, C. T. *Appl. Phys. Lett.* **2004**, *84*, 2649.
(9) Lucas, A. A.; Lambin, P. H.; Smalley, R. E. *J. Phys. Chem. Solids* **1993**, *54*, 587.
(10) Zhao, X.; Liu, Y.; Inoue, S.; Suzuki, T.; Jones, R. O.; Ando, Y. *Phys. Rev. Lett.* **2004**, *92*, 125502.
(11) Zhai, J. P. , Ph.D. Thesis, Hong Kong University of Science and Technology, 2007.
(12) Bennett, J. M.; Richardson, J. W., Jr.; Pluth, J. J.; Smith, J. V. *Zeolites* **1987**, *7*, 160.
(13) Jiang, F. Y.; Zhai, J. P.; Ye, J. T.; Han, J. R.; Tang., Z. K. *J. Cryst. Growth* **2005**, *283*, 108.
(14) Han, B.; Shin, C. H.; Cox, P. A.; Hong, S. B. *J. Phys. Chem. B* **2006**, *110*, 8188.
(15) Mail, G.; Meden, A. *J. Phys. Chem. B* **2002**, *106*, 63.
(16) Li, Z. M.; Zhai, J. P.; Liu, H. J.; Li, I. L.; Chan, C. T.; Sheng, P.; Tang, Z. K. *Appl. Phys. Lett.* **2004**, *85*, 1253.
(17) Subramanian, S.; Mitra, A.; Satyanarayana, C. V. V.; Chakrabarty, D. K. *Appl. Catal. A: General* **1997**, *159*, 229.
(18) Zhai, J. P.; Tang, Z. K.; Lam, F. L. Y.; Hu, X. J. *J. Phys. Chem. B* **2006**, *110*, 19285.

(19) Schnabel, K. H.; Finger, G.; Kornatowski, J.; Elke, L.; Peuker, C.; Pilz, W. *Microporous Mater.* **1997**, *11*, 293.
(20) Parker, L. M.; Bibby, D. M.; Patterson, J. E. *Zeolites* **1984**, *4*, 168.
(21) Nowotny, M.; Lercher, J. A.; Kessler, H. *Zeolites* **1991**, *11*, 454.
(22) Soulard, M.; Bilger, S.; Kessler, H.; Guth, L. *Zeolites* **1987**, *7*, 463.
(23) Zhai, J. P.; Tang, Z. K.; Li, Z. M.; Li, I. L.; Jiang, F. Y.; Sheng, P.; Hu, X. J. *Chem. Mater.* **2006**, *18*, 1505.
(24) Hollmes, A. J.; Kirkby, S. J.; Ozin, G. A.; Young, D. *J. Phys. Chem.* **1994**, *98*, 4677.
(25) During, H. R.; Beshir, W. B.; Gogley, S. E.; Hizer, T.J. J. *Raman Spectrosc.* **1989**, *20*, 311.
(26) Kresse, G.; Furthm; üller, J. *Phys. Rev. B.* **1996**, *54*, 11169.
(27) Perdew, J. P.; Burke, K.; Ernzerhof, M. *Phys. Rev. Lett.* **1996**, *77*, 3865.
(28) Zhao, X.; Liu, Y.; Inoue, S.; Suzuki, T.; Jones, R. O.; Ando, Y. *Phys. Rev. Lett.* **2004**, *92*, 125502.
(29) Sano, N.; Chowalla, M.; Roy, D.; Amaratunga, G. A. *J. Phys. Rev.* **2002**, *66*, 113403.

JP802218X